DOI: 10.1002/ejic.201000563

Patterning Nanoparticles by Microcontact Printing and Further Growth of One-Dimensional Nanomaterials

Lei Ding,[a] Changqing Li,[a] Weiwei Zhou,[a] Haibin Chu,[a] Xiao Sun,[a] Zheng Cao,[a] Zhaohui Yang,[a] Chunhua Yan,[a] and Yan Li*[a]

Keywords: Microcontact printing / Nanoparticles / ZnO / Carbon nanotubes / Nanomaterial arrays

A general method for patterning various functional inorganic nanomaterials on SiO_x/Si substrates by using microcontact printing (μCP) was developed. The application of hydrophobic poly(dimethylsiloxane) (PDMS) stamps is essential for the reproducibility of this process. By tuning the concentration of the nanoparticle solutions, we can control the thickness of the nanoparticle layers on surfaces. The patterned ZnO nanoparticles on surfaces are used as seeds to grow ZnO nanorod arrays, and the patterned Fe_3O_4 nanoparticles or Fe/Mo nanoclusters are used as catalysts for the patterned growth of carbon nanotube arrays. This shows that μCP is a facile method to pattern inorganic nanoparticles relying on PDMS stamps of designed surface affinity. Patterned 1D nanomaterial arrays can subsequently be obtained by use of solution path seeded growth or catalyzed chemical vapor deposition.

Introduction

Functional inorganic nanoparticles (NPs) have been intensively studied as promising materials for future technologies.[1–3] The potential applications highly rely on the assembly and buildup of the NPs.[2,3] To exploit the full functions that nanosystems or nanostructures offer, it is important to develop effective methods for manipulating and patterning NPs.[4] Microcontact printing (μCP), a powerful tool for the preparation of micro- to nanoscaled surface features over distances of centimeters, has gained remarkable popularity in the past decades.[5]

The μCP method was initially used for patterning self-assembled monolayers (SAMs),[6] and now it has become a flexible and versatile method for the micro- and nanofabrication of organic,[7] inorganic,[8] and biological structures.[9] μCP has the advantages of being designable, simple, and clean.[10] However, for patterning inorganic nanomaterials, the surface properties of the poly(dimethylsiloxane) (PDMS) stamps used should be altered to ensure the proper interaction between the nanomaterials and the stamp.[11] The affinity of the NPs to the stamps should be low enough to facilitate the transfer of materials to the target substrates (silicon wafers, glass, quartz, etc.), while the wetting of the stamp by the ink solution should be good enough to ensure the soaking of the ink by the stamps. We previously developed a method for direct fabrication of uniform patterns of iron oxide NPs on the SiO_x/Si surfaces by μCP.[11] Here, we extend the μCP method to the patterning of various functional inorganic NPs, including metallic NPs (Fe, Au), semiconducting NPs (CdS, CdTe, ZnO), magnetic NPs (Fe_3O_4), and polyacid nanoclusters (Fe/Mo nanocluster). Using the patterned NPs on the surface as seeds or catalysts, we successfully fabricated arrays of 1D nanomaterials such as single-walled carbon nanotubes (SWNTs), multiwalled carbon nanotubes (MWNTs), and ZnO nanorods (NRs). Our results show that μCP can be widely used as a convenient tool for the preparation and patterning of 0D or 1D nanomaterials.

[a] Beijing National Laboratory for Molecular Sciences,
State Key Laboratory of Rare Earth Materials Chemistry and Applications,
Key Laboratory for the Physics and Chemistry of Nanodevices,
College of Chemistry and Molecular Engineering, Peking University,
Beijing 100871, P. R. China
Fax: +86-10-6275-6773
E-mail: yanli@pku.edu.cn

Results and Discussion

1. Direct Deposition of Various NPs

μCP has been widely used as a direct patterning method to pattern various functional materials directly on different surfaces. The modified hydrophilic PDMS (normally treated by O_2 plasma) was always used as the stamp for its relatively good soakage of the aqueous solution. But the relatively high surface energy of the PDMS also enhances the force of affinity between the "ink" materials (especially ionic compounds and materials with high polarity) and the stamp, which adds to the difficulty in transporting these materials from the stamp to the substrate. For the inorganic materials, which are normally ionized or highly polarized, we chose hydrophobic PDMS stamps to lower the affinity between the "ink" materials and the stamps.[11] In this way, we were able to pattern various functional inorganic NPs

by the μCP method: for example, CdS, CdTe, ZnO, Fe NPs and Fe/Mo clusters. In the μCP process, the NPs are dissolved in ethanol, which has good soakage for the hydrophobic PDMS stamp and also a high evaporation rate. The preformed NPs are modified onto the PDMS stamp surface uniformly after being dried in air and then deposited onto the SiO_x/Si surface evenly in the following μCP process.

Using this method, we can generate well-organized structures at a large scale. Figures 1A and B show scanning electronic microscopy (SEM) images of the CdS NP patterns fabricated on the SiO_x/Si substrates. The patterns are uniform and well-registered to the design of the stamps. CdTe NPs can also be patterned under similar conditions. Figures 1C and D are the fluorescence images of the patterned CdTe NPs. These images show that the NPs in the patterns still retain their fluorescence. This indicates that μCP is a possible flexible method to pattern fluorescent materials for potential applications in display devices, fake-proof marks, etc.

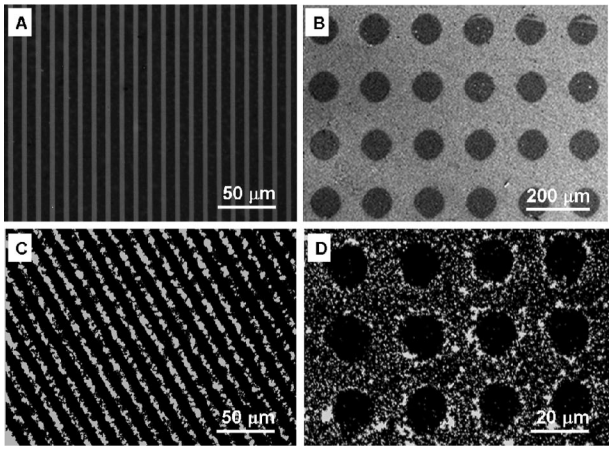

Figure 1. SEM images showing patterns of CdS NPs (A and B) and fluorescence images showing patterns of CdTe NPs (C and D) fabricated on SiO_x/Si substrates by μCP.

We can fabricate patterns of well-dispersed NPs by this method. Relatively low ink concentrations are applied in the μCP process for this kind of NP films. The concentration of the ZnO NPs, Fe NPs, and Fe/Mo clusters is 0.3, 0.2, and 0.2 mM, respectively. Figure 2 shows the patterns of ZnO NPs, Fe NPs, and Fe/Mo clusters fabricated on SiO_x/Si substrates. The SEM images show the macroscale morphology of the patterns, and the high-resolution Tapping Mode (TP) atomic force microscopy (AFM) images clearly present the individually dispersed NPs in the patterns. It should be pointed out that, because of the poor conductivity of the silica layer on top of the SiO_x/Si substrates, the brightness of the features does not represent their height. It shows the charge accumulation when exposed to the electron beam. Actually, the dark stripes in the SEM images correspond to the areas of NPs, and the bright stripes present the substrate surface.

The results in Figures 1 and 2 show that various inorganic NPs or nanoclusters can all be patterned with μCP by using hydrophobic PDMS stamps. The patterns exhibit good registration. The relatively low affinity between the hydrophobic PDMS stamp and NPs is very important for the successful direct deposition of the NPs.

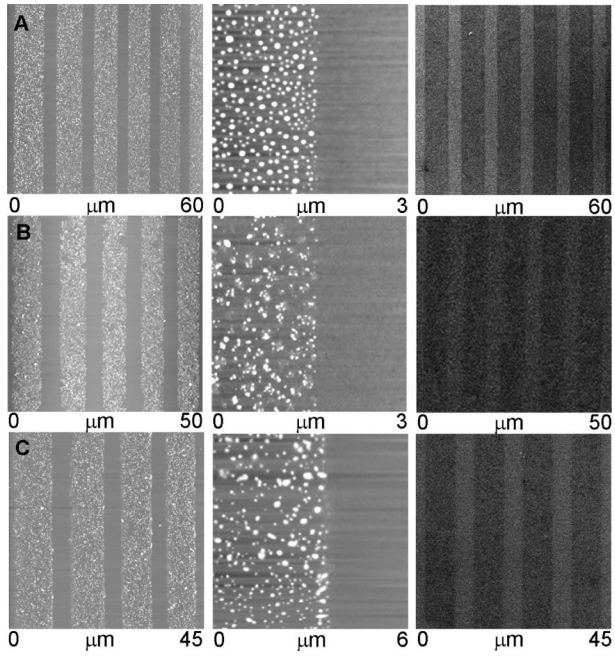

Figure 2. AFM and SEM images showing patterns of ZnO NPs (A), Fe NPs (B), and Fe/Mo clusters (C) fabricated on the SiO_x/Si substrate by μCP. Each middle image is the higher magnification AFM image amplified from the corresponding lower magnification AFM image (left). The images on the right are the SEM images of the NP patterns. The dark stripes in the SEM images correspond to the areas of NPs. The bright stripes present the substrate surface.

2. Effects of Ink Concentration on μCP

In μCP, the ink concentration is always an important factor that affects the resulting patterns. Figure 3 further details the changes in the resulting structures of CdS NPs with increasing ink concentration. The high magnification of the TM-AFM image in Figure 3A shows that the CdS NPs are individually dispersed, with an average height of approximately 5 nm, when the ink concentration is relatively low (ca. 0.2 mM). This average height from the AFM image is similar to the mean size of our CdS nanoparticles measured from TEM images. It can be clearly seen that the edges of the lines are sharp, which means that no obvious material diffusion occurs. When the ink concentration is systematically increased approximately from 0.2 to 5.0 mM, from two (with a height of ca. 10 nm) to more than ten (with a total height greater than 100 nm) layers (Figures 3B–D) are formed on the SiO_x/Si surface. This shows that the height of the resulting structures can be well controlled by tuning the ink concentration.

3. Growth of ZnO NR Arrays

The precise control of the position, spacing, and pattern of the 1D NR or nanowire (NW) arrays is important for

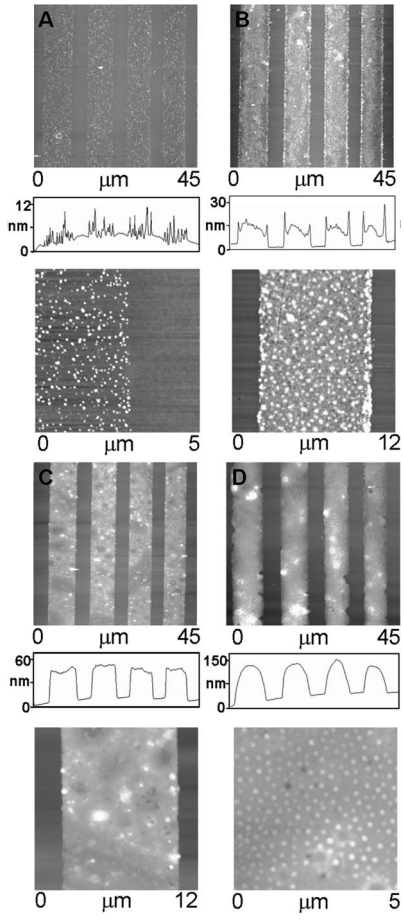

Figure 3. AFM images showing the changes in the resulting structures with increasing ink concentrations of CdS NPs. The ink concentration is 0.2 mM (A), 0.5 mM (B), 2.0 mM (C), 5.0 mM (D), in succession. Each upper image is the AFM image of lower magnification with scanning area of 45 × 45 μm; each middle picture is the cross section profile of the lower-magnification AFM image; each lower image is the AFM image of higher magnification amplified from the corresponding lower-magnification AFM image.

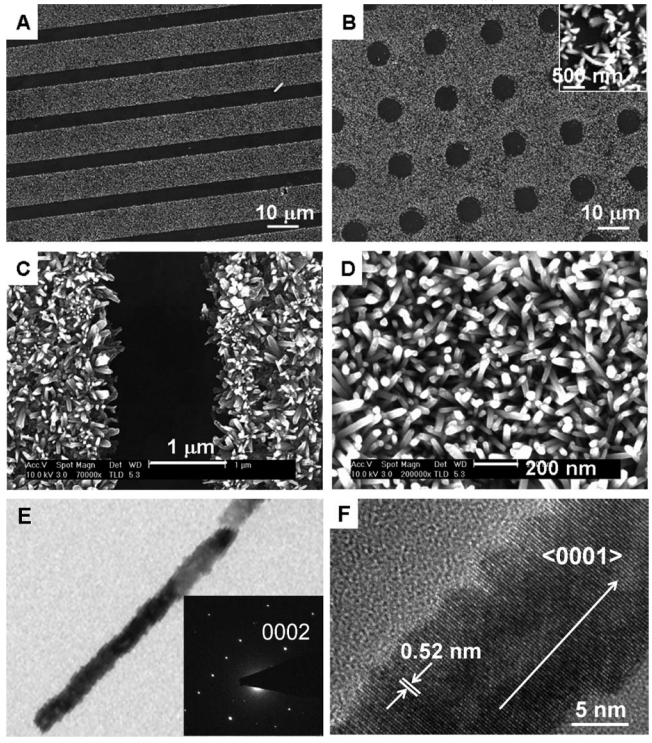

Figure 4. SEM and TEM images showing patterns of ZnO NRs grown from ZnO NPs patterned on the SiO_x/Si surface by μCP. The ink concentration is 0.5 mM (A, B), 2.0 mM (C), 5.0 mM (D), in succession. (E) The TEM image (the inset is the corresponding selected area electron diffraction pattern). (F) The HRTEM image of a NR from the sample shown in D.

further applications. It was reported that some random Au NRs grew from the μCP-patterned Au NPs in solution.[19] Here, we use μCP patterned ZnO NPs as seeds to grow ZnO NR arrays in aqueous solutions of zinc nitrate and methenamine.[18] 1D ZnO nanostructures have important applications in solar cells, gas sensors, lasers, piezoelectric generators, and logic circuits.[20] Herein, we also found that the ink concentration of the ZnO NPs can affect the particle density in the patterns and therefore affect the growth of ZnO NRs. Figures 4A and B show the resulting structures of ZnO NRs when the ink concentration is relatively low (0.5 mM). The formed ZnO NRs are not compact, because of the low density of ZnO NPs deposited by μCP. Also, some of the ZnO NRs do not stand but lie on the surface. With increasing ink concentration (2.0 mM), the density of the resulting ZnO NRs increases (Figure 4C), but the alignment of ZnO NRs is still not very satisfying. High-density and vertically aligned ZnO NR arrays are fabricated on the surface when the ink concentration is increased to 5.0 mM (Figure 4D).

The selected area electron diffraction (SAED) pattern of a NR from the sample shown in D reveals that the NR is a single crystal with the length direction along <0002> (Figure 4E). The high-resolution TEM image of the same NR also shows the well-crystallized structure and the growth direction aligned with the *c* axis. It is found that the growth of NRs is highly site-selective. NRs grow only at the areas where ZnO NPs have been patterned.

Compared with the normally used chemical vapor deposition (CVD) method, which includes evaporation and condensation processes, the growth method of ZnO NRs used here is a low-temperature solution method. It employs preformed ZnO NPs patterned on substrates as the seeds. This not only enables the pattered growth of ZnO NRs, but also avoids the contamination of the products by other elements (the CVD method normally employs metallic NPs as catalysts). Also, it is a large-scale and versatile synthetic process. This approach might find applications in manipulating nanostructured materials for solar energy conversion, light emission, and other promising areas.

4. Growth of Vertically Aligned MWNT Arrays

MWNT arrays are of interest for their potential application in field emission. μCP can be used to pattern catalysts for further growing MWNT arrays. However, normally gel-

like or copolymer-dispersed catalysts are used as inks for their compatibility with plasma-treated PDMS stamps.[21] Here, we demonstrate that by using as-prepared hydrophobic PDMS stamps, Fe_3O_4 NPs can be directly patterned on SiO_x/Si substrates, and then vertically aligned CNT arrays can be fabricated by CVD (Figure 5). The edges of the arrays are regular, and there are no MWNTs growing from the areas where no Fe_3O_4 NPs have been patterned. The Raman spectrum shows that the MWNTs we obtained are of satisfying quality without abundant defects.

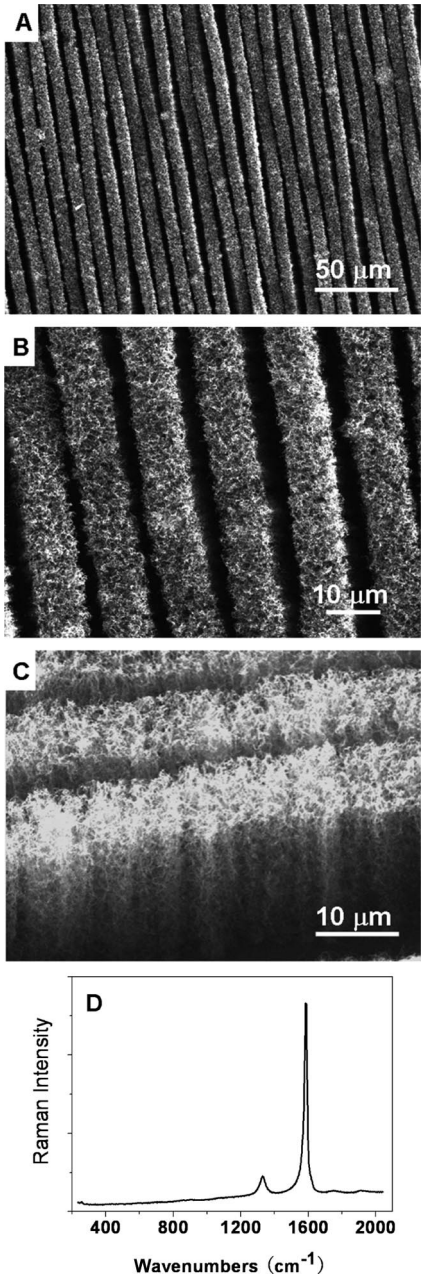

Figure 5. SEM images (A–C) showing patterns of the MWNT array grown from Fe_3O_4 NPs patterned on the SiO_x/Si substrates by μCP: (A, B) Overhead view, and (C) side-view images of the MWNTs array. The periodicity of the array is approximately 10 μm. (D) The Raman spectrum of the produced MWNTs.

The high density of the nanotubes is essential for the vertical alignment of MWNTs. Therefore, it is important to deposit Fe_3O_4 NPs of enough thickness onto the substrate by μCP. When half of the ink concentration was used, fewer Fe_3O_4 NPs were patterned on the substrate, films of lying MWNTs instead of vertically aligned arrays were generated (Figure 6). Our method can easily control the amount of NPs patterned on substrates by altering the concentration of Fe_3O_4 NPs in ethanol solution during the stamp inking process. Our process has another advantage, which is its application without the need for using any surfactants or polymer dispersants. In this way, the introduction of contaminating species, which might influence the growth of MWNTS, is avoided.

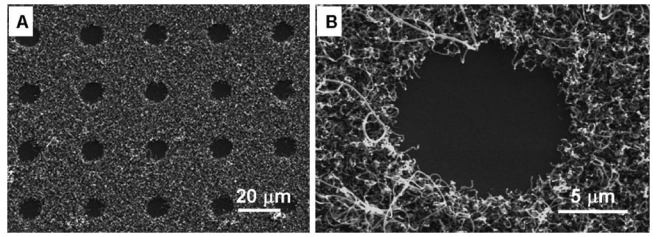

Figure 6. SEM images showing patterns of MWNT film grown from low-concentration Fe_3O_4 NPs patterned on the SiO_x/Si surface by μCP.

5. Growth of Horizontally Aligned SWNT Arrays

Compared with random networks of SWNTs on surfaces, aligned SWNTs can avoid the overlap of nanotubes and the resistance caused by the nanotube junctions. So, horizontally aligned SWNT arrays have been focused on for their wide potential applications in high-frequency submicrometer transistors, radio frequency analog electronics, field-effect transistors, and polarization-sensitive near-field probes.[22] Recently, the surface-lattice-guided growth of SWNTs by CVD has been an important advance in view of its high density and good alignment. Using this method, large-scale, high-density, and well-aligned SWNT arrays have been obtained on single-crystal surfaces including sapphire and quartz.[23] Because the tubes grow tightly on the surface of the substrate, any obstacles on the surface will stop the growth. So it is essential to pattern the catalysts in certain areas and ensure the cleanness of the other areas.

We found that our μCP method can also be used to effectively pattern NPs on quartz substrates. We used our hydrophobic PDMS stamp to pattern Fe/Mo clusters, which have shown to be very good catalysts for the growth of SWNTs,[17] on quartz wafer. The patterned Fe/Mo clusters by the μCP method were then used as catalysts for the growth of well-aligned SWNT arrays on the quartz substrate. Figure 7 shows the SEM image and Raman spectrum of our product. The alignment of the CNTs between the catalyst lines is very good. The density of the arrays is 1–3 SWNTs/μm. The Raman spectrum presented is a typical Raman spectrum of the semiconducting tubes with a radial

breathing mode (RBM) peak at 156 cm^{-1}. This result shows that μCP can be used as a very convenient method to pattern catalysts on quartz substrates for further growth of horizontally aligned SWNT arrays of high density.

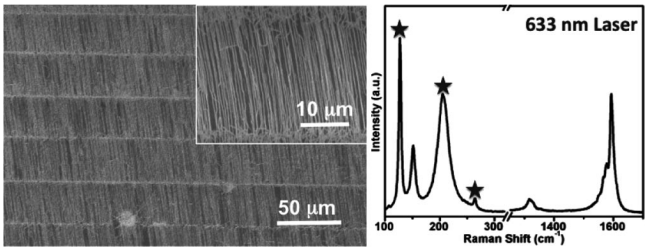

Figure 7. SEM images and Raman spectrum of aligned SWNT arrays grown from μCP-patterned Fe/Mo clusters. The Raman spectrum was recorded with an excitation laser line of 633 nm. The peaks marked with stars correspond to the Raman peaks of the quartz substrate.

Conclusions

Patterned deposition of various functional inorganic NPs, such as CdS, CdTe, ZnO, Fe, Fe_3O_4 NPs and Fe/Mo clusters has been accomplished with μCP by using a hydrophobic PDMS stamp. The hydrophobic PDMS stamp shows good soakage towards ethanol ink solution and compatible weak affinity towards the inorganic NPs. These two issues are crucial for the reliable patterning of inorganic species by the μCP process. The thickness of the patterned features and the dispersion state of the NPs in the features are well controlled simply by altering the concentration of the NPs in the inks. By using the ZnO and Fe_3O_4 NPs patterned by μCP as seeds and catalysts, patterned arrays of vertically aligned ZnO NRs and MWNTs on the SiO_x/Si substrates were prepared. By using patterned Fe/Mo nanoclusters as catalysts, horizontally aligned SWNT arrays on quartz substrates were fabricated. The μCP method proves to be a simple, general, and powerful process for patterning functional inorganic NPs on substrates over large areas. Subsequently, 1D nanomaterial arrays can be prepared by using patterned NPs as seeds or catalysts. This strategy might become a flexible and economic way to fabricate large-area functional nanomaterial patterns for further applications in various fields.

Experimental Section

Preparation of Materials and Substrate: All chemicals used were of analytical grade. Water of Milli-Q quality obtained from the commercially available water purification equipment from Millipore (Bedford, MA) was used throughout the experiments. The p-type Si(111) wafers were cut into 1.0 cm × 1.0 cm pieces. After being ultrasonicated first with ethanol and then with water for 5 min, the wafers were cleaned in piranha solution (H_2SO_4/H_2O_2 = 7:3, v/v) at 100 °C for 30 min and rinsed with water. Then the wafers were dipped in 5% HF solution, rinsed with water, and blown dry with high-purity nitrogen. At last, the wafers were mounted in a furnace at 950 °C for 2.5 h to get clean SiO_x/Si surfaces. The as-prepared PDMS stamps were used with no further treatment except for being cleaned with water and ethanol.

Preparation of Various NPs: CdS NPs capped with mercaptoacetic acid,[12] CdTe NPs capped with 3-mercaptopropionic acid (MPA),[13] ZnO NPs with hydroxy groups on their surfaces,[14] Fe NPs capped with long-chain carboxylic acid and amine groups,[15] Fe_3O_4 NPs with free carboxyl groups on their surfaces,[16] and Fe/Mo clusters[17] were fabricated by using well-established methods according to the corresponding references. The fabricated water-dispersible CdTe NPs were modified with cetyltrimethyl ammonium bromide (CTAB, Sigma, >98%) to improve their solubility in ethanol. The products were diluted by ethanol and used as the "inks" for μCP.

Inking and Printing: Our procedures for patterning various NPs on SiO_x/Si surface with μCP were similar to those in our previous paper.[11] The ink was applied to the stamp by covering the stamp with the ink solution with a pipette and drying in air. Then, the ink was transferred onto the surface of the SiO_x/Si wafer by bringing the stamp into conformal contact with the substrate for 5 min. After the stamp was peeled off, the surface of the substrate was examined with SEM, AFM, and fluorescence microscopy.

Growth of ZnO NR Arrays: ZnO NR arrays were grown by using a simple two-step process.[18] First, ZnO NPs were patterned onto the SiO_x/Si surface by the μCP method. Then, the SiO_x/Si wafer was annealed at 150 °C for 30 min to ensure the adhesion of the particles to the wafer surface. Then, ZnO NRs were grown by suspending the wafer upside-down in an open crystallizing dish filled with an aqueous solution of zinc nitrate hydrate (0.01 M, Beijing Chemical Reagent Co.) and methenamine (0.01 M, Beijing Chemical Reagent Co.) at 85 °C. After reaction for 1 h, the wafer was removed from solution, rinsed with water, and dried.

Growth of MWNT Arrays: MWNTs arrays were synthesized by chemical vapor deposition (CVD). Three steps were inevitable in the procedure. Firstly, the SiO_x/Si wafer patterned with Fe_3O_4 NPs by μCP was placed in a quartz tube reactor and heated to 750 °C at a speed of 30 °C min^{-1} under a 30 Torr flow of Ar. Then, the flow of Ar was shut down, and H_2 (40 Torr) was introduced to reduce Fe_3O_4 NPs for 10 min, after which the pressure of H_2 was reduced to 20 Torr, and C_2H_2 (100 sccm) together with Ar (30 Torr) were introduced into the reactor to carry out CVD for 20 min at 750 °C. Finally, the system was cooled down to room temperature under the flow of Ar.

Growth of Aligned SWNT Arrays: The substrates for the CVD approach were ST-cut single-crystal quartz wafers (36° Y-cut) obtained from Hoffman Materials Inc. used without any further treatment. Ethanol (200 proof 99.5%) was purchased from Fisher Scientific and used for the catalyst solutions and carbon precursors in bubblers. Methanol (99.9% pure) was purchased from Fisher Scientific and used for the carbon precursors in bubblers. The growth experiments were performed in a 1 inch tube furnace at 900 °C. Typically, the substrate with catalyst precursor deposited on it was annealed in air at 750 °C for 10 min. Then, the substrate was heated up to 800 °C and kept for 15 min with a flow of hydrogen (750 sccm), followed by CVD growth of SWNTs at 900 °C under a flow of hydrogen (500 sccm) and argon (300 sccm through a methanol bubbler and 150 sccm through an ethanol bubbler). After 15 min of growth, the sample was cooled to room temperature and inspected with SEM and Raman spectroscopy.

Characterization: A SPA400 scanning probe microscope (SPM, Seiko Instrument Inc.) equipped with a 100 μm scanner was used for AFM imaging, and all topographic images were recorded with

a TM-AFM instrument. A SEM (FEIXL30 S-FEG, operated at 10 kV) instrument was used to characterize the morphology of the products. A fluorescence microscope (Leika DMLM) equipped with a CCD instrument (Cool SNAP, Roper Scientific) was used to observe the luminescence of patterned CdTe NPs on Si wafer. The Raman spectrometer used in the experiments is a LabRam ARAMIS from Horiba Jobin Yvon with an excitation laser line of 633 nm wavelength. The excitation radiation was polarized parallel to the aligned SWNTs during the Raman spectroscopic measurements. The laser power was carefully controlled to avoid any heating effects.

Acknowledgments

We thank Dr. Su Guo and Prof. Xinsheng Zhao for their help in fluorescence microscopy studies. This work was supported by the National Natural Science Foundation of China (Project 50772002) and the Ministry of Science and Technology of China (Projects 2006CB932403, 2007CB936202, and 2006CB932701).

[1] a) J. J. Hickman, D. Ofer, P. E. Laibinis, G. M. Whitesides, M. S. Wrighton, *Science* **1991**, *252*, 688–691; b) R. Elghanian, J. J. Storhoff, R. C. Mucic, R. L. Letsinger, C. A. Mirkin, *Science* **1997**, *277*, 1078–1081; c) M. Bruchez Jr., M. Moronne, P. Gin, S. Weiss, A. P. Alivisatos, *Science* **1998**, *281*, 2013–2016; d) V. L. Colvin, M. C. Schlamp, A. P. Alivisatos, *Nature* **1994**, *370*, 354–357; e) W. U. Huynh, X. Peng, A. P. Alivisatos, *Adv. Mater.* **1999**, *11*, 923–928.

[2] V. M. Rotello, *Nanoparticles: Building Blocks for Nanotechnology*, Kluwer Academic/Plenum Publishers, New York, **2004**, pp. 1–27.

[3] Z. L. Wang, *Characterization of Nanophase Materials*, Wiley-VCH, Weinheim, **2000**.

[4] B. D. Gates, Q. B. Xu, M. Stewart, D. Ryan, C. G. Willson, G. M. Whitesides, *Chem. Rev.* **2005**, *105*, 1171–1196.

[5] Y. N. Xia, G. M. Whitesides, *Angew. Chem. Int. Ed.* **1998**, *37*, 551–575.

[6] J. C. Love, L. A. Estroff, J. K. Kriebel, R. G. Nuzzo, G. M. Whitesides, *Chem. Rev.* **2005**, *105*, 1103–1170.

[7] a) D.-G. Choi, H. K. Yu, S.-M. Yang, *Mater. Sci. Eng. C* **2004**, *24*, 213–216; b) M. Wang, H.-G. Braun, T. Kratzmuller, E. Meyer, *Adv. Mater.* **2001**, *13*, 1312–1317; c) H.-W. Li, B. V. O. Muir, G. Fichet, W. T. S. Huck, *Langmuir* **2003**, *19*, 1963–1965.

[8] a) Z. Wang, J. Yuan, J. Zhang, R. Xing, D. Yan, Y. Han, *Adv. Mater.* **2003**, *15*, 1009–1012; b) Z. Zheng, O. Azzaroni, M. E. Vickers, T. S. Huck, *Adv. Mater.* **2006**, *18*, 805–811.

[9] a) A. Bernard, J. P. Renault, B. Michel, H. R. Bosshard, E. Delamarche, *Adv. Mater.* **2000**, *12*, 1067–1070; b) S. A. Lange, V. Benes, D. P. Kern, J. K. H. Hoerber, A. Bernard, *Anal. Chem.* **2004**, *76*, 1641–1647; c) J. P. Renault, A. Bernard, D. Juncker, B. Michel, H. R. Bosshard, E. Delamarche, *Angew. Chem. Int. Ed.* **2002**, *41*, 2320–2323.

[10] a) X. C. Wu, A. M. Bittner, K. Kern, *Adv. Mater.* **2004**, *16*, 413–417; b) V. Santhanam, R. P. Andres, *Nano Lett.* **2004**, *4*, 41–44; c) X. C. Wu, L. F. Chi, H. Fuchs, *Eur. J. Inorg. Chem.* **2005**, 3729–3733; d) X. C. Wu, S. Lenhert, L. F. Chi, H. Fuchs, *Langmuir* **2006**, *22*, 7807–7811.

[11] L. Ding, W. W. Zhou, H. B. Chu, Z. Jin, Y. Zhang, Y. Li, *Chem. Mater.* **2006**, *18*, 4109–4114.

[12] T. Vossmeyer, G. Reck, L. Katsikas, E. T. K. Haupt, B. Schulz, H. Weller, *Science* **1995**, *267*, 1476–1479.

[13] L. L. Yang, Z. H. Yang, W. X. Cao, L. Chen, J. Xu, H. Z. Zhang, *J. Phys. Chem. B* **2005**, *109*, 11501–11504.

[14] a) D. W. Bahmenann, C. Kormann, M. R. Hoffmann, *J. Phys. Chem.* **1987**, *91*, 3789–3798; b) N. S. Pesika, Z. Hu, K. J. Stebe, P. C. Searson, *J. Phys. Chem. B* **2002**, *106*, 6985–6990.

[15] Y. Li, J. Liu, Y. Q. Wang, Z. L. Wang, *Chem. Mater.* **2001**, *13*, 1008–1014.

[16] J. Park, K. An, Y. Hwang, J.-G. Park, H.-J. Noh, J.-Y. Kim, J.-H. Park, N.-M. Hwang, T. Hyeon, *Nat. Mater.* **2004**, *3*, 891–895.

[17] L. An, J. Owens, L. McNeil, J. Liu, *J. Am. Chem. Soc.* **2002**, *124*, 13688–13689.

[18] C. Q. Li, Z. Jin, H. B. Chu, Y. Li, *J. Nanosci. Nanotechnol.* **2008**, 4441.

[19] A. J. Mieszawska, F. P. Zamborini, *Chem. Mater.* **2005**, *17*, 3415–3420.

[20] a) M. Law, L. E. Greene, J. C. Johnson, R. Saykally, P. D. Yang, *Nat. Mater.* **2005**, *4*, 455; b) Q. Wan, Q. H. Li, Y. J. Chen, T. H. Wang, X. L. He, J. P. Li, C. L. Lin, *Appl. Phys. Lett.* **2004**, *84*, 3654; c) M. H. Huang, S. Mao, H. Feick, H. Q. Yan, Y. Y. Wu, H. Kind, E. Weber, R. Russo, P. D. Yang, *Science* **2001**, *292*, 1897; d) Z. L. Wang, J. H. Song, *Science* **2006**, *312*, 242; e) W. Park, J. S. Kim, G. C. Yi, H. J. Lee, *Adv. Mater.* **2005**, *17*, 1393.

[21] a) H. Kind, J. M. Bonard, C. Emmenegger, L. O. Nilsson, K. Hernadi, E. Maillard-Schaller, L. Schlapbach, L. Forro, K. Kern, *Adv. Mater.* **1999**, *11*, 1285–1289; b) H. Kind, J. Bonard, L. Forro, K. Kern, L. Nilsson, L. Schlapbach, *Langmuir* **2000**, *16*, 6877–6883; c) A. M. Cassell, S. Verma, L. Delzeit, M. Meyyappan, J. Han, *Langmuir* **2001**, *17*, 260–264; d) R. D. Bennett, A. J. Hart, A. C. Miller, P. T. Hammond, D. J. Irvine, R. E. Cohen, *Langmuir* **2006**, *22*, 8273–8276.

[22] a) C. Kocabas, S. Dunham, Q. Cao, K. Cimino, X. Ho, H. S. Kim, D. Dawson, J. Payne, M. Stuenkel, H. Zhang, T. Banks, M. Feng, S. V. Rotkin, J. A. Rogers, *Nano Lett.* **2009**, *9*, 1937–1943; b) C. Kocabas, H. S. Kim, T. Banks, J. A. Rogers, A. A. Pesetski, J. E. Baumgardner, S. V. Krishnaswamy, H. Zhang, *Proc. Natl. Acad. Sci. USA* **2008**, *105*, 1405–1409; c) Q. Cao, H. S. Kim, N. Pimparkar, J. P. Kulkarni, C. Wang, M. Shim, K. Roy, M. A. Alam, J. A. Rogers, *Nature* **2008**, *454*, 495–500; d) E. Cubukcu, F. Degirmenci, C. Kocabas, M. A. Zimmler, J. A. Rogers, F. Capasso, *Proc. Natl. Acad. Sci. USA* **2009**, *106*, 2495–2499.

[23] a) C. Kocabas, S. J. Kang, T. Ozel, M. Shim, J. A. Rogers, *J. Phys. Chem. C* **2007**, *111*, 17879–17886; b) S. J. Kang, C. Kocabas, T. Ozel, M. Shim, N. Pimparkar, M. A. Alam, S. V. Rotkin, J. A. Rogers, *Nat. Nanotechnol.* **2007**, *2*, 230–236; c) L. Ding, D. N. Yuan, J. Liu, *J. Am. Chem. Soc.* **2008**, *130*, 5428–5429; d) W. Zhou, C. Rutherglen, P. J. Burke, *Nano Res.* **2008**, *1*, 158–165; e) L. Ding, A. Tselev, J. Y. Wang, D. N. Yuan, H. B. Chu, T. P. McNicholas, Y. Li, J. Liu, *Nano Lett.* **2009**, *9*, 800–805; f) L. Ding, W. Zhou, T. P. McNicholas, J. Y. Wang, H. B. Chu, Y. Li, J. Liu, *Nano Res.* **2009**, *2*, 903–910.

Received: May 21, 2010
Published Online: August 17, 2010

